

# A Preliminary Ribbon Climber Design with Focus on Tribology and Fatigue

Larry Bartoszek, P.E.  
Bartoszek Engineering  
design@bartoszekeng.com

## Abstract

*This paper will outline an independent ribbon climber design for the first construction climber on the space elevator. Principals of this design procedure will be applicable to a climber of any mass, and the intent of the design is to be scalable. The design will use the baseline climber mass distribution outlined in “The Space Elevator” by Edwards and Westling as a starting point, but the details of the traction mechanism differ fundamentally from that shown in the book for reasons described.*

*Overall dimensions of the elevator ribbon shown in the book will also be assumed. The paper will focus on two possible failure modes of the wheels and axles of the drive train driven by tribological and fatigue considerations that will have to be overcome in a successful climber design.*

*A complete preliminary design is not possible at this time because critical pieces of information about the mechanical properties of the CNT ribbon material are not known. However, estimates can be made of the impact on the design of parameters having possible ranges of values, such as the coefficient of friction between the traction drive and the ribbon.*

## 1. Design Assumptions

This paper will focus on the design of the traction drive and associated structural components of the first construction climber for the space elevator as outlined in “The Space Elevator—a revolutionary Earth-to-space transportation system,” by Edwards and Westling. The basic design of the traction mechanism shown in this paper differs fundamentally from the track and roller system in the book. The traction drive shown here is a pinched-wheel design with two wheels forced against the ribbon and each other to achieve traction with the ribbon.

The design of the ribbon climber in this paper assumes the mass distribution from Table 3.2 of “The Space Elevator”.

One goal of the paper is to determine if this preliminary design is within the combined mass budget shown in the table of less than 233 kg. (The entire structure budget cannot be consumed by the traction drive system.)

**Table 1: Mass distribution of components of the first construction climber**

| Component   | Mass (kg) |
|---|-----------|
| Ribbon  | 520       |
| Attitude Control                                    | 18        |
| Command   | 18        |
| Structure   | 64        |
| Thermal Control                                     | 36        |
| Ribbon Splicing                                     | 27        |
| Power Control                                       | 27        |
| Photovoltaic Arrays<br>(12 m <sup>2</sup> , 100 kW) | 21        |
| Motors (100 kW)                                     | 127       |
| Track and Rollers                                   | 42        |
| TOTAL   | 900       |

A simplified system model is shown in Figure 1. The design starts with the minimal configuration of just two wheels. Criteria will be given for when additional pairs of wheels will be required. The transmission shown in Figure 1 is a placeholder because if a motor can be found that has the desired torque-speed curve, a direct drive is preferred. If a transmission is found to be necessary, the efficiency of the drive will be degraded by the presence of mechanical gearing. Not shown is a brake to allow the

climber to stop at any altitude without requiring power to the motors.

The photovoltaic array that powers the motors is not shown in the block diagram, but is assumed.

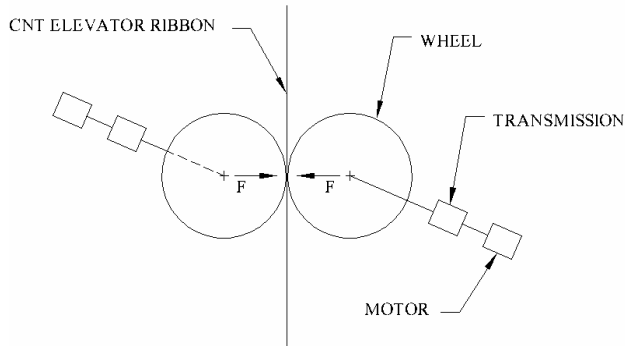


**Figure 1: Block diagram of the proposed climber system. F is the force pinching the wheels to the ribbon to produce traction.**

The wheels, axles and structure of the climber in this design are initially assumed for the purpose of this paper to be made from Aluminum 6061-T6. There are several reasons for this. First, this alloy of aluminum is a readily available alloy commonly used in aerospace applications. It is commercially available in almost every form. It has excellent welding, forging and cutting properties. This author has greater familiarity with the fatigue characteristics of this alloy than those of other candidates such as steels, titanium and magnesium, but a detailed comparison needs to be made in the final design to choose the best material.

### 1.1 Why are tribology and fatigue important considerations in climber design?

The space elevator is 100,000 km long. The construction climbers must make it out to the end of the ribbon with as close to 100% confidence of a successful trip as practical. The climbers must not have a failure that could damage the ribbon or prevent the next climber from continuing to augment the ribbon. The simplest calculation one can do is to look at the total number of times a wheel must rotate to get to the end of the ribbon. If we assume a 20 inch diameter wheel (.508 m), the circumference of the wheel is 62.831 inches (1.596 m). This means that this wheel must rotate almost 63 million times to make it to the end of the ribbon. This is far up the S-N curve for any non-ferrous material. If the wheel were half that diameter, it would need to rotate twice as many times, or 126 million cycles.

Rolling means fully reversed stress cycles in the axle and the contact surface of the wheel. Fully reversed stress is the most severe type of stress leading to fatigue failure. Many non-ferrous alloys do not even report fatigue strengths for greater than  $10^7$  cycles.

This paper will focus on two types of component failures associated with fatigue that could lead to catastrophic failure of the climber or damage to the ribbon. First, the axles will be analyzed as beams in bending due to the force required to hold the wheels to the ribbon. It will be shown that this force is inversely proportional to the coefficient of friction between the ribbon and wheel. If the actual coefficient of friction between the wheels and ribbon is below a certain value, there may not be a real engineering material for the axles strong enough to avoid fatigue cracking before the end of the climb.

The wheel mating surface will also be analyzed for sub-surface stresses due to traction and the compression holding the wheel to the ribbon. This type of fatigue failure could lead to chunks of metal separating from the contact surface of the wheel and potentially puncturing the ribbon during subsequent revolutions of the wheel.

Tribology is the study of friction, lubrication and wear. The first climber has many of the mechanical characteristics of an electric automobile, only made much more complicated by the effects of vacuum and extremes of temperature from exposure to space. Climbers must be able to survive a variety of earthly conditions while they are still in the atmosphere, as well as perform as a spacecraft once they have left the atmosphere. Wheels and axles require bearings to mate with the non-rotating components of the climber structure. To quote reference [2], "The warning must be never to use a ball-bearing in a space mechanism without the guidance of a space tribology expert." The design shown here will use as placeholders various common mechanical components such as bearings with the understanding that they will be replaced in the final design with space-worthy versions.

Tribological considerations are the first reasons to favor a pinched wheel design over a tracked climber traction drive. If a pinched wheel version can be made to work it will inherently have fewer pieces than a tracked version. The track represents a significant research and development effort to come up with a material and design that can flex as frequently as a climber drive requires. The simplest tracked drive is shown in figure 1b. In a sense, the problem of traction is doubled in the simplest tracked design because the inner surface of the track must develop traction with the drive rollers, as well as getting traction between the elevator ribbon and track. Existing tracked drives such as in tanks rely on a sprocket to drive the track with mating teeth around the inside of the track. The flexing of the track, the meshing of teeth or the

friction between the rollers and track are all tribological issues that are irrelevant in the pinched wheel design.

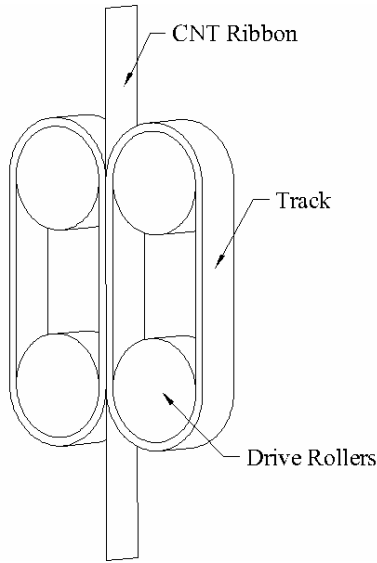


**Figure 1b: Sketch of the simplest traction drive system. The tracks would be pinched together by forces on the wheels as in the pinched-roller design.**

## 2. The mathematical model of the drive train and the motivation to eliminate the track from the track and roller drive

A free body diagram of a wheel is shown in Figure 2.

Defining terms in Figure 2:

$R$  = radius of the wheel

$N$  = normal force between ribbon and wheel

$F$  = applied force compressing wheel to ribbon

$T$  = applied torque from drive train

$m_c$  = mass of the climber

$f$  = friction force between ribbon and wheel

$g(r)$  = gravitational drag force expressed as a function of  $r$ , radius from the center of the Earth

$$g(r) = \frac{M_e \cdot G}{r^2} - r \cdot \omega^2$$

$G$  = Newton's gravitational constant

$$G = 6.67 \cdot 10^{-11} \cdot \frac{\text{m}^3}{\text{sec}^2 \cdot \text{kg}}$$

$M_e$  = mass of the Earth

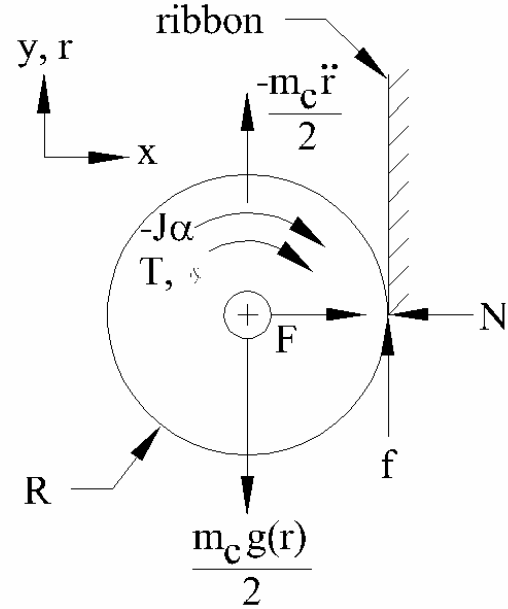


**Figure 2: Free Body Diagram of a wheel**

$$M_e = 5.9788 \cdot 10^{24} \cdot \text{kg}$$

$\omega$  = angular velocity of the Earth about its axis

$$\omega = 7.2929 \cdot \frac{10^{-5}}{\text{sec}}$$

$J$  = rotary moment of inertia of wheel

$\alpha$  = rotational acceleration of wheel,  $\text{sec}^{-2}$

$\ddot{r}$  = linear acceleration along ribbon

$x, y$  = Cartesian coordinates,  $y$  along ribbon,  $x$  perpendicular to face of ribbon

$\theta$  = Angle of rotation around the axis of the wheel, radians

In applying d'Alembert's Principle to the wheel, for convenience the moment is summed about the point of contact between the wheel and ribbon. This eliminates the friction force, the wheel compressive force and the normal force from the equation.

$$\sum M = T - \frac{m_c \ddot{r} R}{2} - \frac{m_c g(r) R}{2} - J \alpha = 0 \quad (1)$$

The contact is assumed to be rolling and not sliding, so the linear and angular positions, velocities and accelerations are related by the following expressions:

$$r = R \theta,$$

$$\dot{r} = R \dot{\theta} \text{ and}$$

$$\ddot{r} = R \ddot{\theta} = R \alpha$$

These expressions are used to eliminate the angular acceleration term from equation 1. (This model neglects the finite size of the zone of contact between the wheel and ribbon as discussed below.)

Rearranging the terms of equation 1 and making the appropriate substitutions gives an equation for the torque required to accelerate the climber upwards with any given linear acceleration  $\ddot{r}$ :

$$T = \ddot{r} \left( \frac{J}{R} + \frac{m_c R}{2} \right) + \frac{m_c g(r) R}{2} \quad (2)$$

This equation shows that for the climber to accelerate at a given acceleration, the larger the rotary moment of inertia is, the more torque is required.  $J$  is the only term in this equation that can be varied by design selections. The mass of the climber is determined by the requirements of the elevator and the force of gravity is determined by the altitude of the climber on the ribbon.

Every effort must be made to reduce the rotary moment of inertia of the drive train because the torque required to raise the climber is directly proportional to the power required. If the power is fixed at a constant value, then increasing  $J$  lowers the maximum acceleration of the climber. In other calculations performed by the author and available at

[www.bartoszekeng.com/se\\_calcs/ribbon\\_climber.htm](http://www.bartoszekeng.com/se_calcs/ribbon_climber.htm), the acceleration attainable by the construction climbers assuming an initial laser power of 100 kW gives longer trip times than those quoted in *The Space Elevator* even before  $J$  is factored in. The rotary moment of inertia of the climber drive will directly impact the time (and thus the budget) it takes to bring the elevator on-line for business.

This is another motivation to look at a climber design that has no track. The track adds to  $J$  without contributing to the traction. As will be seen below, the traction comes from the pinch force between the roller pairs. This effect is also true in the track and roller design as shown in figure 1b. The minimal track and roller design has two roller pairs to circulate the track around. The track in-between the end roller pairs is not being compressed against the ribbon, compression only comes near the rollers. The track in-between roller pairs cannot contribute significantly to the total traction making it superfluous and deleterious to the design.

### 3. The effect of estimated coefficients of friction between the ribbon and wheels

One of the numbers critical to the design of the climber to be determined by experiment once a sufficient quantity of ribbon fabric is made is the coefficient of friction between the fabric and the material of the wheel in contact with the ribbon. Other important mechanical properties

are the strength of the CNT fabric to resist the compressive stress caused by the pinched wheels and the wear properties that can be expected to lead to material being transferred from the wheel to the ribbon.

The friction model used here is Coulomb dry friction in which the traction does not depend on the area of contact, but only on the normal force and coefficient of friction as given by

$$f = \mu N \quad (3)$$

where  $\mu$  is the coefficient of friction.  $\mu$  may have different values depending on whether the contact is sliding (kinetic friction) or not sliding (static friction). The case of sliding contact is considered a failure of the climber's traction, so the kinetic coefficient of friction will not be used in this analysis. Climbers must operate in the regime up to the point of impending sliding and no further, so anytime the coefficient of friction appears in an equation, it is understood to be the static coefficient of friction.

The first calculation looks at the static case where the wheel is stationary on the ribbon and the applied torque is just the braking torque required to keep the climber from rolling down the ribbon. In this case the inertial terms all go to zero.

By summing the forces in the x and y directions, we get the relationship between the weight of the climber, the force applied to compress the wheels together and the friction force available for traction.

$$\sum F_y = f - \frac{m_c g(r)}{2} = 0 \quad (4)$$

$$\sum F_x = F - N = 0 \quad (5)$$

Rearranging (4) gives

$$f = \frac{m_c g(r)}{2} \quad (6)$$

The traction force between the ribbon and the wheel is equal to half the weight of the climber. Rearranging (5) gives  $F = N$ , the normal force coming from the second wheel in the wheel pair (through the ribbon) is balanced by the applied force on the first wheel.

Equation (6) describes the condition in which the weight of the climber is balanced by the friction force, but the friction force required is less than that calculated by equation (3). The condition of *impending sliding* is required to allow equation (3) to be used with equation (6). Substituting  $F$  for  $N$  in (3) gives  $f = \mu F$  which gives

$$F(\mu) = \frac{m_c g(r)}{2\mu} \quad (7)$$

In the case of a stationary climber, the amount that the wheels must be compressed together to get just enough friction to hold the climber in place is directly proportional to half the weight of the climber (assuming the weight is evenly distributed on both wheels) and inversely proportional to the coefficient of friction between the wheel and ribbon. This compressive force on the wheel must be considered a minimum and a conservative design will allow for the application of a higher force on the wheels.

Looking at the case of the climber starting out near the surface of the earth,  $m_c = 900 \text{ kg}$  and  $g(r) = 9.8 \text{ m/sec}^2$ . The force required to hold up the climber drops off as gravity does with altitude, so the highest force necessary to support the climber is near the surface of the earth.

The theoretical range of values for the coefficient of friction is from zero to infinity, but the range encountered in normal practice is much more limited. Values of friction greater than 1.0 are possible but generally imply some sort of adhesion between the contacting surfaces and are not usual in the context of rolling contact. Typical coefficients of friction for dry bearing materials are from .01 to .1. A wide variety of engineering materials have coefficients that lie in the range between .1 and 1.0.

Figure 3 shows a graph of the force required between wheels as a function of the coefficient of friction. The force values are given in pound force (lbf).

If the measured friction coefficient is found to be near a typical value like .1, then the force required on the wheel to be at the point of impending sliding is about ten thousand pounds or five tons for the lightest climber. This force has a significant impact on the axles of the wheels and bounds the size of the actuators that apply this force to the axles. A measured value for  $\mu$  significantly less than .1 will have a deleterious effect on the design, effectively making the ribbon too slippery for traction climbing.

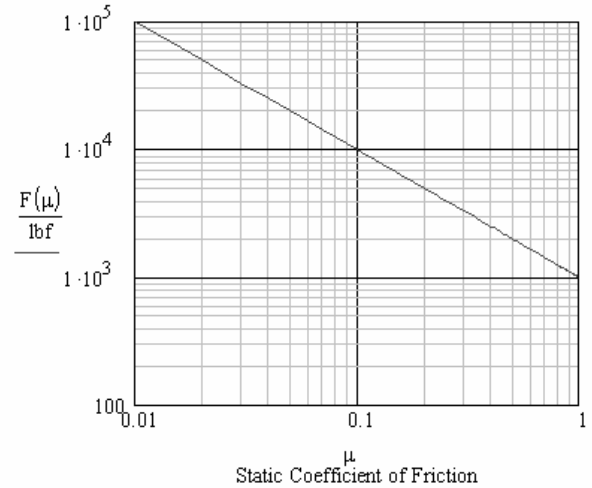


**Figure 3: Graph of Force required between wheels (lbf) vs. coefficient of friction for the first construction climber.**

#### 4. Analyzing the axles as cantilever beams

The width of the pilot ribbon is widest at GEO and is calculated to be slightly less than 14 inches wide (35.5 cm). The actuators that compress the wheels around the ribbon must be outside the widest part of the ribbon and sufficiently far away from its edge that they would never scrape the edge of the ribbon. A reasonable first guess at the length of an axle from the center of the first climber's wheel would be 14 inches. This shaft can be modeled as a cantilever beam with one end fixed to the center of the wheel and the other free. The force applied to the wheel calculated above is evenly distributed on the axle on both sides of the wheel, so the force the axle shaft on one side of the wheel sees is half the total force on the wheel.

The maximum bending stress in a cantilever occurs at the base of the cantilever next to the fixed end constraint. This stress is calculated from:

$$f_b = \frac{M \cdot R_{axle}}{I_{xx}} \quad (8)$$

where:

$f_b$  = bending stress at point of maximum bending moment, psi

$M$  = maximum bending moment, lbf-in

$M = F_{axle} l$

$l = 14 \text{ in}$ , the length of the cantilever

$$F_{axle} = \frac{F(.1)}{2} \quad (\mu = .1 \text{ assumed})$$

$$F_{axle} = 4.96 \times 10^3 \text{ lbf}$$

$R_{axle}$  = radius of the axle, inches

$I_{xx}$  = area moment of inertia of the shaft cross-section, in<sup>4</sup>

$$I_{xx} = \frac{1}{4} \cdot \pi \cdot (R_{axle})^4$$

For the axle shaft model as described, the maximum bending stress at the base of the cantilever can be expressed as a function of the axle radius. Figure 4 shows a graph of the bending stress as a function of axle radius.

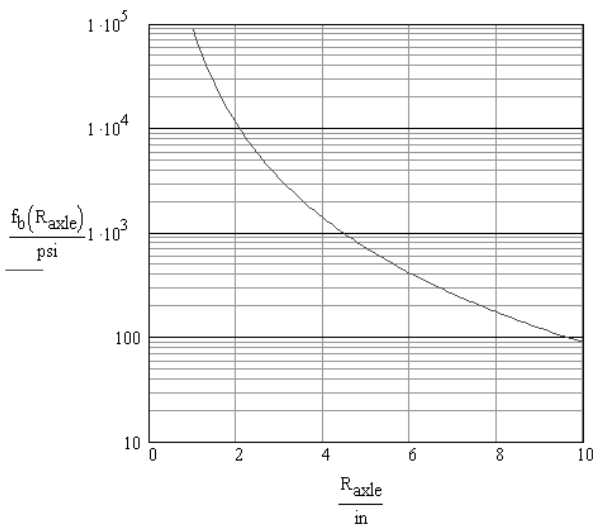


**Figure 4: Graph of maximum axle bending stress (psi) vs. axle radius (in) for  $\mu = .1$**

For a complete stress analysis, the bending stress must also be combined with the torsional stress due to the braking and driving torques. Calculating the torsional stress requires detailed knowledge of the acceleration profile of the climber which is not complete as of this writing. This calculation is just a quick estimate of the minimum size of the wheel axle required just to absorb the pinch-force between the wheels.

To find the minimum axle radius, the calculated bending stress must be compared against an allowable stress for fatigue. Most sources quote allowable stresses for fatigue at 50% confidence to failure. This means that if a device is run at the quoted stress level there is a 50% chance of component failure by fatigue after the quoted number of stress cycles. The usual fatigue allowable for fully reversed bending in Al 6061-T6 is given as 14 ksi at  $5 \times 10^7$  stress cycles. As stated earlier, 50% confidence is unacceptable. The author has performed an extensive

fatigue analysis on a pulsed power device for the MiniBooNE experiment at the Fermi National Accelerator Laboratory in Batavia, IL. In unpublished work the conservative stress allowable calculated for 97.5% confidence was found to be 6.5 ksi for cycle life greater than  $10^8$  cycles of fully reversed stress in Aluminum 6061-T6. If this is used as the allowable stress in the graph in Figure 4, then the axle radius must be larger than 2.4 inches.

If the coefficient of friction between the wheel and ribbon were experimentally found to be .01 instead of .1, the force required on the axle would be 10 times greater and the stress would be 10 times greater. The axle radius would then have to be larger than 5.15 inches to avoid fatigue failure. This corresponds to a 10.3 inch diameter shaft passing through a 20 inch diameter wheel. Coefficients of friction below .01 would eventually force the shaft to be larger in diameter than the wheel, an absurdity.

Another important check on the condition of the axle shaft is to calculate its deflection. This deflection causes the end of the shaft to have both an angular and transverse offset from the nominal central axis of the shaft. In the final design of the climber a shaft coupling will need to be selected that can absorb angular and transverse offsets without introducing backlash into the system.

Assuming  $\mu = .1$  and the force required at this friction level, the deflection of a 2.4 inch radius shaft 14 inches long is calculated from the following:

$$d_{max} = \frac{F_{axle} \cdot l^3}{3 \cdot E_{al} \cdot I_{xx}} \quad (9)$$

where:

$d_{max}$  = maximum deflection of the end of the shaft

$$F_{axle} = 4.96 \times 10^3 \text{ lbf}$$

$$E_{al} = 10.3 \times 10^6 \text{ psi}$$

$$I_{xx} = 26.1 \text{ in}^4 \text{ (for } R_{axle} = 2.4 \text{ in)}$$

which gives a maximum shaft deflection of :

$$d_{max} = .017 \text{ in}$$

This deflection may be large enough to choose deflection as the sizing criterion for the shaft once the complete stress criterion is satisfied. If the fatigue strength of the shaft is found to be adequate for a particular radius but the deflection is too large to accommodate in the drive train, the shaft would have to be made larger to limit the deflection to an acceptable value.

From a design strategy perspective, if the stress in the axle had proven too great given the assumed friction coefficient, the only solution given the free body diagram of the wheel is to lower the weight of the climber a wheel pair must carry. Since the mass of the climber is determined by other considerations and cannot be arbitrarily reduced, the way to lower the load on a wheel pair is to add more wheel pairs and assume they can carry the weight of the climber equally distributed between them. (This strategy is similar to that of freight trains where additional engines are added as the number of rail cars increases.) A climber with more than a single wheel pair has a significant increase in the complexity of the torque control system, hence the focus on the simplest traction drive system.

The conclusion from this analysis is that at a coefficient of friction of .1 or greater, a single roller pair can be compressed together with a force that generates sufficient traction with the ribbon, and an axle shaft size can probably be found that satisfies a complete fatigue stress criterion. The next calculation will look at whether this wheel compressive force is low enough to avoid fatigue spallation of the rolling surface of the wheel.

## 5. Calculating Hertzian contact stress in the wheels and the area of contact

The first comment to be made about this subject is that the study of the stress state in the zone of contact between two solid bodies is very complex. A rigorous and complete analytical treatment of the sub-surface stress in the wheels is far larger than this paper can report. What will be presented is a shortcut based on contact mechanics and the maximum shear stress theory that is useful in design to bound the nature of the problem. The final design of the drive train will involve a lengthy finite element analysis of the wheels and axles to insure the design against failure.

Maximum shear stress theory gives the condition that the maximum shear stress must be less than or equal to half of the tensile yield stress of the material to avoid shear failure. In fatigue, this condition is modified by replacing the tensile yield stress with the fatigue allowable stress which is always a lower number. Mathematically this is expressed as:

$$\tau_{\max} \leq \frac{\sigma_f}{2} \quad (10)$$

where:

$\tau_{\max}$  = maximum shear stress

$\sigma_f$  = fatigue stress allowable = 6.5 ksi

When two cylinders whose axes are parallel are in contact and pressed together, the zone of contact changes from a line parallel to the central axes to a flattened

rectangular area as the material of the wheels elastically deforms from the force of contact. Figure 5 introduces a new coordinate system to describe the zone of contact. The half-width of the zone of contact is designated by  $b$ , and is shown greatly exaggerated in size with respect to the diameter of the cylinders.

The stress state in the zone of contact changes as traction is applied, but a useful number is the maximum pressure in the zone for the case without traction. The maximum pressure occurs at the origin of the coordinate system shown in figure 5 and is calculated from:

$$p_o = \frac{2 \cdot F}{\pi \cdot b \cdot l} \quad (11)$$

where:

$p_o$  = maximum pressure at the origin of the zone of contact

$F$  = force between the two wheels =  $9.921 \times 10^3$  lbf for  $\mu = .1$

$b$  = half width of the zone of contact

$l$  = length of the contact zone parallel to the axis of the wheels = 6 inches for the first climber

The equation for  $b$  for the case of two cylinders of equal diameter and made of the same material is:

$$b = \left[ \frac{2 \cdot F \cdot d}{\pi \cdot l} \cdot \frac{(1 - \nu^2)}{E_{al}} \right]^{\frac{1}{2}} \quad (12)$$

where:

$d$  = initial guess value for the diameter of the wheel = 20 in

$\nu$  = Poisson's ratio for aluminum = .334

This equation completely neglects the contribution of the ribbon fabric to the stress state in the zone of contact. This was considered reasonable given the thin-ness of the ribbon fabric and the lack of information about its modulus and Poisson's ratio. Experimentation is needed to validate this assumption.

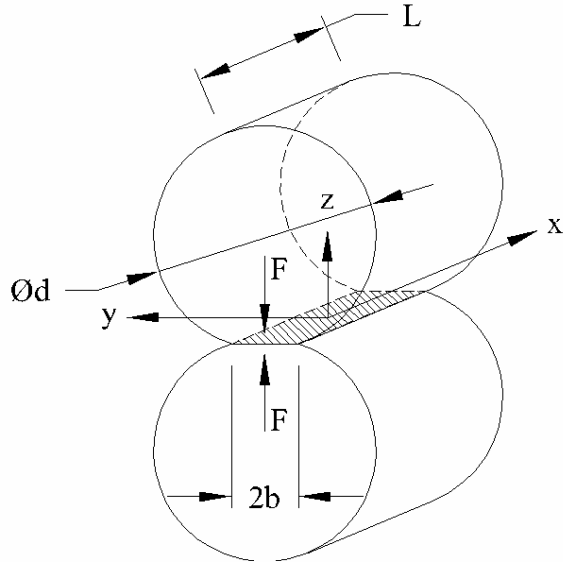


**Figure 5: Sketch of two identical cylinders in contact. The hatched area is the flattened zone of contact.**

Given the above values to evaluate the equations,  $b$  and  $p_o$  are found to be:

$$b = .043 \text{ in} \quad \text{and} \quad p_o = 24.7 \text{ ksi}$$

As discussed in reference [9], the maximum shear stress in the zone of contact occurs below the surface and is the  $\tau_{yz}$  component. Its value maximizes at  $b$  inches below the surface of contact and is given as:

$$\tau_{\max} = .3p_o \quad (13)$$

which evaluates to:

$$\tau_{\max} = 7.41 \text{ ksi}$$

Applying maximum shear stress theory as shown in equation 10,

$$\sigma_f/2 = 3.25 \text{ ksi}$$

The condition of equation 10 is violated because the calculated maximum shear stress is 2.28 times greater than the allowable shear stress. If we apply the 50% confidence value for the fatigue allowable, or 14 ksi, then the shear stress allowable would still only be 7 ksi, less than the calculated allowable. This indicates that there would be a greater than 50% chance of a surface spallation failure at  $5 \times 10^7$  revolutions of the wheels, if the wheels are 20 inches in diameter and made of aluminum alloy 6061-T6.

There are several possible ways to bring the maximum pressure in the zone of contact down. From inspection of equation 11, the force could be reduced or the size of the zone of contact could be increased. The length of the rollers or the half-width of the zone could be increased to increase the area of the zone. Increasing the length of the rollers past the width of the ribbon would complicate the determination of the amount of the force between the wheels actually being transmitted to the ribbon for the development of traction. To avoid this complication, all of the calculations below use the length of the wheels as 6 inches.

Keeping all other factors such as the force and the length the same, we see that  $b$  is directly proportional to the square root of the diameter of the wheels. To reduce the pressure by a factor of 2.28, the wheels would have to increase in diameter by a factor of almost 5.2, making them 104 inches in diameter.

Another possible solution would be to change the material of the rim of the wheel in contact with the ribbon. An advantage of a ferrous alloy over a non-ferrous one is that the ferrous alloys have endurance limits. If the stress can be kept below a given value, the fatigue life becomes effectively infinite. For example, the 50% confidence endurance limit for stainless steel 321 is 38 ksi. The confidence analysis on this alloy has not been done by this author, but if we assume that the scatter in the data for this stainless steel is similar to that of the aluminum alloy, we can estimate the 97.5% confidence level for the stainless by applying the same reduction factor to the stainless as seen in the aluminum alloy. This would give a fatigue allowable for stainless 321 as:

$$\sigma_f = \sigma_{f50} \frac{6.5}{14}$$

or

$$\sigma_f = 17.64 \text{ ksi}$$

The appropriate constants for stainless steel in the equations for  $b$  and  $p_o$  are:

$$E_{st} = 29 \times 10^6 \text{ psi}$$

$$\nu_{st} = .292$$

Evaluating equations 11 and 12 for stainless 321, the maximum shear stress is found to be 8.8 ksi, matching the shear allowable, when the wheel diameter is 38.6 inches. The guess value for the wheel diameter of 20 inches is still too low because Young's modulus is three times larger for stainless steel than that of aluminum, driving down the half-width of the zone of contact.

The problem becomes one of finding the minimum mass solution. Instead of changing the material, another solution is to increase the number of wheel pairs pinching the ribbon. This has the effect of reducing the force on

the wheels by a factor of 2 for a second set of wheels, 3 for a third and so on, assuming that the load of the climber can be equally distributed on multiple wheel pairs.

The actual wheels will be designed to have as little mass as possible to reduce the total rotary moment of inertia and mass of the drive. However, to compare different configurations of numbers of wheel pairs and wheel material, a useful comparison is to treat the wheels as solid cylinders and calculate the total mass of the wheel sets. Selecting from these results can prune the design space.

The results for six different configurations which all satisfy the condition of equation 10 are summarized in Table 2.

An interesting result from Table 2 is that the maximum contact pressure stays the same as long as the material is not changed between configurations. From equations 11 and 12, if  $F$  is reduced by a factor  $N$  and  $d$  is also reduced by the same factor, then  $b$  is reduced by  $N$ . Equation 11 shows that the result of these reductions cancels and the pressure is a constant. If the contact pressure is an issue for the ribbon fabric, the way to reduce the pressure is to choose a wheel material of lower Modulus of Elasticity.

**Table 2: Comparison of six different wheel configurations**

| Wheel material | No. of wheels | Diameter of wheels, in. | Total mass of wheels <sup>1</sup> , kg, $\times 10^3$ | $p_c$ , ksi |
|----------------|---------------|-------------------------|---|-------------|
| Al 6061-T6     | 2             | 104                     | 4.528   | 10.83       |
| Al 6061-T6     | 4             | 52                      | 2.266   | 10.83       |
| Al 6061-T6     | 6             | 34.66                   | 1.510   | 10.83       |
| SS 321         | 2             | 38.6                    | 1.847   | 29.4        |
| SS 321         | 4             | 19.3                    | 0.92  | 29.4        |
| SS 321         | 6             | 12.87                   | 0.62  | 29.4        |

<sup>1</sup>Wheels modeled as solid cylinders, not practical wheel designs.

The conclusion from this analysis is that if the ribbon can stand the contact pressure shown, the minimum mass configuration would be three pairs of stainless steel rollers.

Trying to reduce the mass of the drive further by adding another pair of stainless rollers will reduce the diameter to the point where the number of revolutions required to get to the end of the ribbon exceeds  $10^8$  revolutions, the edge of the fatigue data. Also, the rotational velocity of the wheels increases as the diameter decreases for a given linear velocity of the climber on the ribbon. This effect adds dynamic stress components that have to be taken into

account in the fatigue analysis of the wheel and the maximum speed capability of the motors and other drive elements. At a climber cruising speed of 200 km/hr, the wheels in the three-pair stainless drive train are rotating at 3246 RPM.

The three-pair stainless rollers may work out to be practical in the sense that the force required for traction is greatest near the earth's surface where the speed of the climber is lowest. Once the pull of gravity drops off as the climber gains altitude, the force pinching the ribbon can be reduced to reduce the stress in the zone of contact. Subsurface stresses caused by increased traction requirements at lower altitudes will trade off with dynamic stresses as the wheel rotates faster at higher altitudes. Only a complete acceleration profile and wheel stress analysis will answer some of the open questions.

The mass shown for any of the wheel configurations is far greater than the budgeted mass for the climber's traction drive system of less than 233 kg. The next question to address is whether a simplified wheel design (short of a complete optimization analysis) can fit within the mass budget.

Going back to the axle analysis, if there are two pairs of wheels the force on the axles is reduced by a factor of 2. Redoing that calculation gives an axle shaft diameter of 3.78 inches. Using this number, the simplified wheel layout can be created as shown in Figure 6. Other dimensions in the wheel drawing are educated first guesses.

The mass of the wheel shown in figure 6 is 59.6 kg. A drive train with four of these wheels has a mass of 238.4 kg, still above the target before the mass of any other component is included.

Three pairs of wheels reduces the force on the axles further and allows the axles' diameter to become 3.31 inches. Figure 7 shows the layout for the three-pair simplified wheel.

The mass of the wheel shown in figure 7 is 35.5 kg. Six of these wheels add up to 213 kg. This number is still too large for the mass of the wheels alone. Given the masses of the axles, compression actuators, couplings and structures required to hold the climber together, the wheels have to be reduced in mass considerably before the climber mass budget can be satisfied.

## 6. Conclusion

The conclusion to draw from this analysis is that the total mass of the drive train from these simplified calculations and conceptual designs is not orders of magnitude too high, but it will require a lot of detailed analysis and creative design work to package the drive train into the desired mass budget. The same considerations of fatigue and traction apply to the rollers of the track and roller drive. If it is this difficult to get a

pinched roller drive within the desired mass budget of the climber, the track and roller design is even more difficult.

Before this work can be finalized, experimental data on the coefficient of friction between the ribbon and various roller materials is necessary.

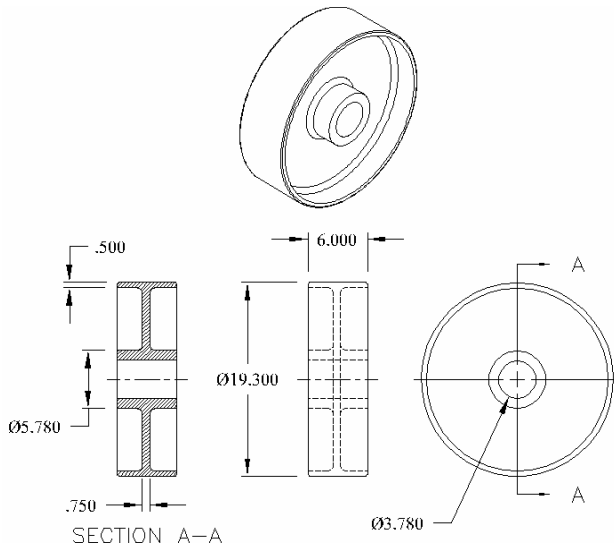


**Figure 6: Simplified wheel layout for the two-pair stainless wheel climber drive. All dimensions in inches.**

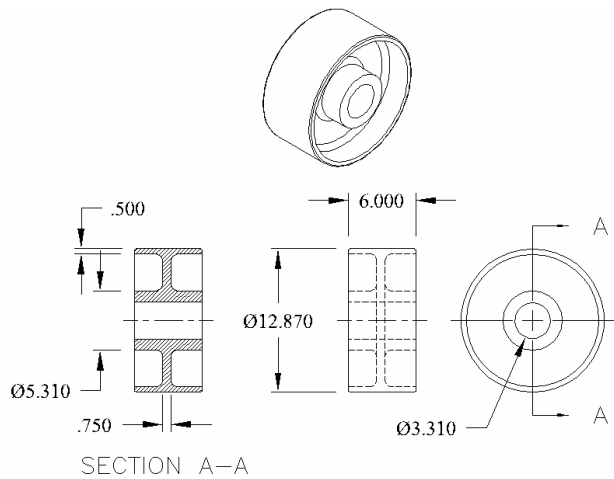


**Figure 7: Simplified wheel layout for the three-pair stainless wheel climber drive. All dimensions in inches.**

## References

- [1] Edwards, B. and Westling, E. (2003) *The Space Elevator—a revolutionary Earth-to-space transportation system*, BC Edwards, Houston.
- [2] Fortescue, P. and Stark, J. (1995) *Spacecraft Systems Engineering*, Wiley, Chichester.
- [3] Johnson, K. (1985) *Contact Mechanics*, Cambridge University Press, Cambridge.
- [4] Shigley, J. (1977) *Mechanical Engineering Design*, McGraw-Hill, New York.
- [5] Mabie, H. and Ocvirk, F. (1978) *Mechanisms and Dynamics of Machinery*, Wiley, New York.
- [6] Bharat, B. and Gupta, B. (1991) *Handbook of Tribology—Materials, Coatings and Surface Treatments*, McGraw-Hill, New York.
- [7] Ogata, K. (1978) *System Dynamics*, Prentice-Hall, New Jersey.
- [8] Weichel, H. (1990) *Laser Beam Propagation in the Atmosphere*, SPIE, Washington.
- [9] Shigley, J. and Mischke, C. (1986) *Standard Handbook of Machine Design*, McGraw-Hill, New York.
- [10] Boyer, H. (1986) *Atlas of Fatigue Curves*, ASM International, Ohio.
- [11] Lampman, S. (1996) *ASM Handbook Volume 19 Fatigue and Fracture*, ASM International, Ohio.